

Reduction of the Optical Losses in CdTe/ZnTe Thin-Film Solar Cells

S. CHUSNUTDINOW^a, R. PIETRUSZKA^a, W. ZALESZCZYK^a, V.P. MAKHNIY^b, M. WIATER^a,
V. KOLKOVSKY^a, T. WOJTOWICZ^a AND G. KARCZEWSKI^a

^aInstitute of Physics, PAS, al. Lotników 32/46, 02-668 Warszawa, Poland

^bYuri Fedkovych Chernivtsi National University, 2 Kotsyubynsky Str., 58012 Chernivtsi, Ukraine

We report on reduction of optical losses in *n*-CdTe/*p*-ZnTe thin-film solar cells grown by molecular beam epitaxy. The investigated thin-film devices were grown from elemental sources on monocrystalline, semi-insulating, (100)-oriented GaAs substrates. The optical losses have been reduced by a texturing of the device surface and by depositing of a ZnO antireflection coating. Current-voltage and spectral characteristics of the investigated *p*-ZnTe/*n*-CdTe solar cells depend significantly on the preparation of the surface of the ZnTe window. We describe a procedure of chemical etching of the ZnTe window leading to surface texturing. A ZnO layer of proper thickness deposited by low-temperature atomic layer deposition technique on the ZnTe surface forms an effective antireflection coating that leads to the reduction of optical losses. Due to reduction of the optical losses we observe increase of the short-circuit current, J_{SC} , by almost 60% and of the energy conversion efficiency by 44%.

DOI: [10.12693/APhysPolA.126.1072](https://doi.org/10.12693/APhysPolA.126.1072)

PACS: 81.15.Hi, 73.61.Ga, 85.60.Dw, 88.40.jm

1. Introduction

The interest in application of solar cells for industrial electricity production has been increasing rapidly in recent years. The main goal of many research groups for the nearest future is to improve the efficiency of Si cells from the current efficiency of 22% [1] to the maximum theoretical efficiency of 29% [2] and of CdTe/CdS cells from the current efficiency of 16% [1] to the maximum theoretical efficiency of 28% [3]. There are many reasons for the reduced energy conversion efficiency of the nowadays solar cells. They are related to optical, electrical and recombination losses. The optical losses are due to the surface reflection, reflection from the rear surface of the cell and shading by top electrical contact. There are two well-known methods of reducing optical losses: minimization of the size of top contact and deposition of antireflection coatings (ARC) on the device surface. For different solar cell devices different thin films are used as ARC, including: TiO₂, ITO, Al₂O₃, SiO₂, SiN_x, MgF₂ and ZnO [4–8]. The reflection can also be reduced by surface texturing. Textured surfaces have an advantage of a light-trapping due to their reduced reflection and increased optical path length in reflection or absorption. The solar cells can be textured using a photolithographic technique [9], chemical and electrochemical etching [10, 11] and reactive ion etching (RIE) [12, 13].

Here, we report on our attempt to reduce optical losses by the either surface texturing or formation of ARC on the top of *n*-CdTe/*p*-ZnTe thin-film solar cells grown by molecular beam epitaxy (MBE).

2. Experimental

The investigated *p*-ZnTe/*n*-CdTe heterostructures were grown by MBE on semi-insulating, (100)-oriented

GaAs substrates in ultrahigh vacuum EPI 620 MBE system. Firstly, a 13 μm thick, highly iodine doped *n*-type CdTe buffer was grown at the reduced substrate temperature of about 250 °C, with the purpose of increasing electron concentration. The best contact layers grown this way exhibited carrier concentrations around 10¹⁹ cm⁻³. The *n*-CdTe buffer was then covered by 2 μm thick, undoped CdTe and subsequently by 1.5 μm of nitrogen-plasma doped *p*-type ZnTe. For the growth of the intrinsic CdTe and *p*-type ZnTe the growth temperature was elevated to 30 °C.

Surface texturing of the top ZnTe layer was done by electrochemical etching in acidic solution composed of HNO₃:HCl:H₂O at a mixing ratio of 1:4:20. During the etching process the structure with top side contact to ZnTe made of Au constituted anode and another electrode was made of platinum wire. Various voltages between electrodes, from 0.5 V to 2 V, were applied during process. After etching the samples were rinsed in deionized water, dipped in a solution of polysulfide to remove oxidation products, and then rinsed again in de-ionized water [14]. In order to produce antireflection coatings and transparent contacts the Al-doped ZnO (AZO) thin-films were grown by atomic layer deposition (ALD) technique in a Savannah-100 reactor (Cambridge NanoTech). For the growth diethylzinc (Zn(C₂H₅)₂) and water vapor were used as zinc and oxygen precursors, respectively. For doping with aluminum, trimethylaluminum (TMA) was used. Growth temperature was 160 °C.

The thickness of ZnO films was measured by a Mikropack NanoCalc 2000 reflectometer. The thickness of the antireflection films was around 100 nm. ZnO were deposited on the untreated surface of the structures. Gold ohmic contacts to *n*-ZnO were deposited by e-beam evaporation (in PREVAC 190 System). Prior to

the formation of ohmic contact to the n -type CdTe layer the top-most layers of ZnO, ZnTe, and intrinsic CdTe were removed by etching in Br-methanol. The contact was formed by In soldering to the exposed n -type CdTe buffer. Photovoltaic response was measured using a source-meter Keithley 2601 with Solar Simulator LS0308 class A, at illumination irradiance of 100 mW/cm^2 . Data processing was performed using Software package Tracer 2 ReRa Solutions. Quantum efficiency was measured using a PV quantum efficiency system (185–1100 nm; SPE-QUEST system, ReRa Solutions).

3. Results and discussion

3.1. Morphological study and optical characterization

Figure 1 shows the typical scanning electron microscopy (SEM) image of a surface etched at +1 V. During the etching process the current was time dependent. We observe a strongly corrugated surface structure with etch pits of different sizes and forms. The size of etch pits varies from 50 nm to 200 nm (Fig. 1a,b). For etching times longer than 40 s the surface becomes covered by very fine needles with diameters of several nm (see Fig. 1c,d). For further studies we used samples etched for 40 s and having on the surfaces etch pits of size 150–200 nm.

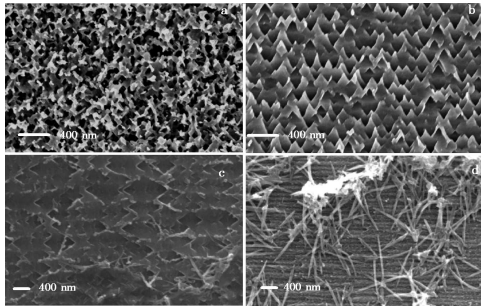


Fig. 1. SEM image of the top p -ZnTe layer that was electrochemically etched at +1 V in $\text{HNO}_3\text{:HCl:H}_2\text{O}$ solution for the period of: (a) 20 s, (b) 40 s, (c) 60 s, (d) 80 s.

The results of the measurement of quantum efficiency of the etched structure is presented in Fig. 2, and compared with that of unprocessed structure and structure covered by ZnO antireflective coating (see further). As can be seen in Fig. 2, surface modification by electrochemical etching does not increase quantum efficiency noticeably.

The next approach to reduce optical losses was ALD deposition of thin AZO film on the top surface of the solar cells. Additional advantage of the AZO films is that they are very good candidates for transparent contacts. That is because they are known to be highly conductive and their optical transparency in a wide spectral region exceeds 90% [15]. The refractive index of AZO (1.954) is

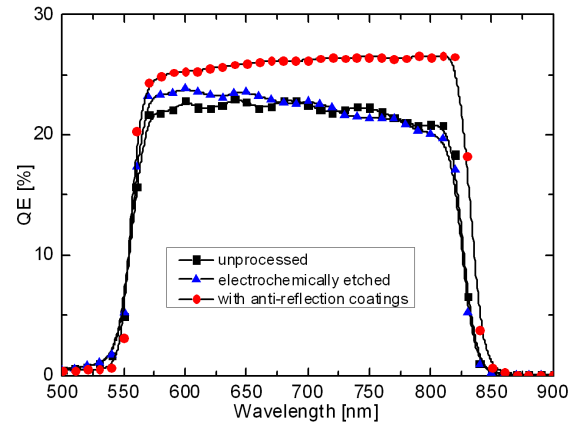


Fig. 2. Quantum efficiency as a function of wavelength measured at room temperature for three typical CdTe/ZnTe solar cells: one unprocessed and two after our attempts to reduce optical losses.

smaller than the refractive indexes of both ZnTe (2.835) and CdTe (2.968) at 820 nm. Because of this, the AZO films reduce the reflectance of CdTe/ZnTe solar cells from 20% down to 2% at 820 nm [16]. As a result the external quantum efficiency increases by almost 5% in the absorption range of CdTe, as can be seen in Fig. 2. Another effect of antireflection coating is the disappearance of the Fabry–Perot oscillation, also visible in Fig. 2.

3.2. Solar cells properties

Figure 3 shows the J – V characteristic for the three types of CdTe/ZnTe solar cells, used in these studies. They can be well described by the diode Shockley equation for real solar cells with the parasitic resistances

$$J = J_0 \left(\exp \left(\frac{q(V - JR_S)}{nkT} \right) - 1 \right) + \frac{V - JR_S}{R_{Sh}} - J_{Ph}, \quad (1)$$

where J_{Ph} is the photocurrent, J_0 is the dark saturation current and n is the diode ideality factor (which depends on the current flow mechanism), R_S the series resistance, and R_{Sh} is the shunt resistance. To a first approximation the R_S and R_{Sh} can be determined from the slopes of the J – V curve at $V = V_{OC}$ and $J = J_{SC}$, respectively. Here V_{OC} is an open circuit voltage and J_{SC} is a short circuit current. The open-circuit voltage, V_{OC} , is the maximum voltage available from a solar cell, and this occurs at zero current. The short-circuit current, J_{SC} , is the current through the solar cell when the voltage across the solar cell is zero. R_{Sh} is represented by the slope at J_{SC} . Typically, the resistances at J_{SC} and at V_{OC} determined from data curve in Fig. 3 and to show in Table. From Eq. (1) we obtain the open circuit voltage by setting $J = 0$ and $R_{Sh} \gg R_S$:

$$J_{Ph} \approx J_{SC} \approx J_0 \left(\exp \left(\frac{qV_{OC}}{nkT} \right) - 1 \right). \quad (2)$$

Hence

$$\ln(J_{SC}) = \ln(J_0) + \frac{qV_{OC}}{nkT}. \quad (3)$$

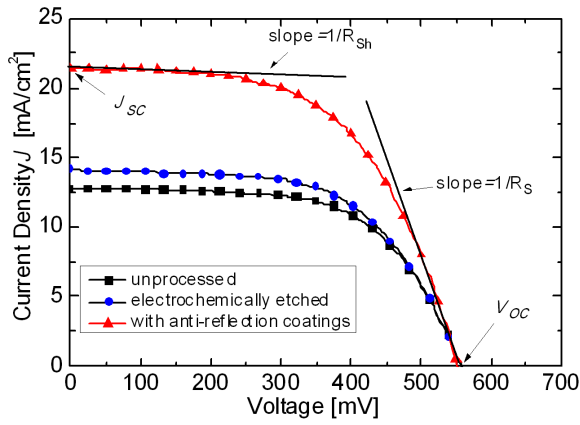


Fig. 3. Typical $J - V$ characteristics of various types of CdTe/ZnTe solar cells collected under illumination of $100 \text{ mW} \cdot \text{m}^{-2}$.

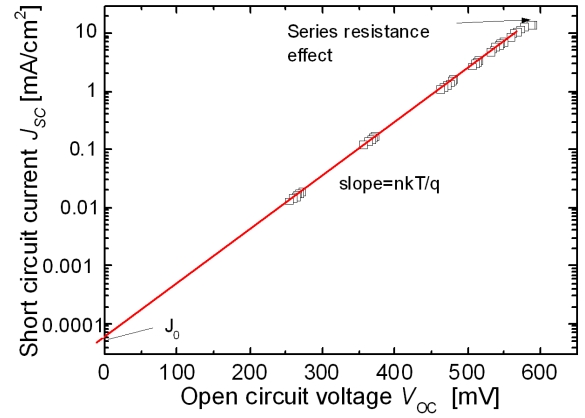


Fig. 4. Short-circuit current versus open-circuit voltage illustrating the method of parameters extraction for unprocessed structure.

TABLE I

Average series resistance (R_S), shunt resistance (R_{Sh}), open circuit voltage (V_{OC}), short circuit current (J_{SC}), fill factor (FF) and efficiency (η) for CdTe/ZnTe solar cells. These photovoltaic parameters were measured under AM 1.5 illumination at 100 mW cm^{-2} at 300 K. 1 — structure without any processing toward reduction of optical losses, 2 — structure that was electrochemically etched, 3 — structure with antireflection coatings.

	J_{SC} [mA/cm ²]	V_{OC} [mV]	FF [%]	η [%]	R_{Sh} [$\Omega \cdot \text{cm}^2$]	R_S [$\Omega \cdot \text{cm}^2$]	J_0 [mA/cm ²]	n
1	12.77	556.3	61.5	4.4	893	11	6.02×10^{-5}	1.8
2	13.89	555.4	59.5	4.6	567	10	5.7×10^{-5}	1.7
3	21.48	552.0	56.6	6.7	690	6.8	2.8×10^{-5}	1.5

Using this equation, the values of n and J_0 can be determined from the measured values of J_{SC} and V_{SC} at different levels of illumination, as presented in Fig. 4 for the unprocessed structure. The results of such procedure are presented in Table together with other parameters, as described in the caption. Determined ideality parameter n is in the range from 1 to 2, and the saturation J_0 current varies in the range of 10^{-4} – 10^{-5} mA/cm² at 300 K, which is typical for this type of diodes [17]. The value of the diode ideality factor indicates that the dominant carrier recombination in the space charge region takes place on the deep-level defects with the hole activation energy 0.78 eV and concentration $\approx 10^{13} \text{ cm}^{-3}$. Most probably these defects are created due to the CdTe/ZnTe lattice mismatch [18]. It can be seen in Fig. 3 that the $J-V$ curve under illumination for structure that was electrochemical etched showed small change in comparison to $J-V$ curve for unetched structure. Figure 3 shows also the $J-V$ curve of the solar cell that was antireflection coated. We observe that the current density J_{SC} increases by almost 60% and that the efficiency increases by 44%, from 4.5 to 6.5%. The V_{OC} does not change. The average photovoltaic parameters are presented in Table.

4. Conclusions

We have found that in the CdTe/ZnTe solar cells the optical losses can be reduced much more efficiently by depositing of antireflection coatings than by surface texturing produced via electrochemical etching with $\text{HNO}_3:\text{HCl}:\text{H}_2\text{O}$. Even after optimal electrochemical etching procedure we observed the etch pits with sizes, in the range 50-200 nm, which are too small to reduce reflectance. On the other hand, all four important solar cell parameters such as short circuit current density (J_{SC}), efficiency (η), ideality factor (n) and series resistance (R_S) improve when the ZnO layers are deposited on the top surface of solar cells. An increase of relative current density by 60% and of efficiency by 44% was observed.

Acknowledgments

This work was supported by the European Union within the European Regional Development Fund through the Innovative Economy grant MIME (POIG.01.01.02-00-108/09).

References

- [1] M.A. Green, K. Emery, Y. Hishikawa, W. Warta, E.D. Dunlop, *Prog. Photovolt Res. Appl.* **22**, 1 (2014).
- [2] A. Richter, M. Hermle, S.W. Glunz, *IEEE J. Photovolt.* **3**, 1184 (2013).
- [3] A.L. Fahrenbruch, R.H. Bube, *Fundamentals of Solar Cells: Photovoltaic Solar Energy Conversion*, Academic Press, New York 1983.
- [4] H. Mackel, R. Ludemann, *J. Appl. Phys.* **92**, 602 (2002).
- [5] M. Barrera, J. Pla, C. Bocchi, *Sol. Energy Mater. Sol. Cells* **92**, 1115 (2008).
- [6] G. Zhang, J. Zhao, M.A. Green, *Sol. Energy Mater. Sol. Cells* **51**, 393 (1998).

- [7] S.I. Muramatsu, T. Uetmatsu, H. Ohtsuka, Y. Yazawa, T. Warabisako, H. Nagayoshi, K. Kamisako, *Sol. Energy Mater. Sol. Cells* **65**, 599 (2001).
- [8] Y.F. Makableh, R. Vasan, J.C. Sarker, A.I. Nusr, S. Seal, M.O. Manasreh, *Solar Energy Mater. Solar Cells* **123**, 178 (2014).
- [9] J.A.W. Zhao, X. Dai, M.A. Green, S.R. Wenham, in: *22nd IEEE PV Specialists Conf.*, 1991, p. 399.
- [10] E. Vazsonyi, K. de Clercq, R. Einhaus, E. van Kerschaver, K. Said, J. Poortmans, J. Szlufcik, J. Nijs, *Sol. Energy Mater. Sol. Cells* **57**, 179 (1999).
- [11] M.J. Sailor, in: *Porous Silicon in Practice: Preparation, Characterization and Applications*, Wiley-VCH Verlag, Weinheim 2011, p. 5.
- [12] T. Wells, M.M. El-Gomati, J.J. Wood, *J. Vac. Sci. Technol. B* **15**, 397 (1997).
- [13] J. Yoo, Kyunghae Kim, M. Thamilselvan, N. Lakshminarayn, Young Kuk Kim, Jaehyeong Lee, Kwon Jong Yoo, Junsin Yi, *J. Phys. D: Appl. Phys.* **41**, 125205 (2008).
- [14] F. Zenia, C. Lévy-Clément, R. Triboulet, R. Könenkamp, K. Ernst, M. Saad, M.C. Lux-Steiner, *Appl. Phys. Lett.* **75**, 531 (1999).
- [15] G. Luka, T.A. Krajewski, B.S. Witkowski, G. Wisz, I.S. Virt, E. Guziewicz, M. Godlewski, *J. Mater. Sci. Mater. Electron.* **22**, 1810 (2011).
- [16] <http://filmetrics.com/reflectance-calculator>.
- [17] S. Chusnutdinow, V.P. Makhniy, T. Wojtowicz, G. Karczewski, *Acta Phys. Pol. A* **122**, 1077 (2012).
- [18] G. Karczewski, S. Chusnutdinow, K. Olender, T. Wosiński, T. Wojtowicz, *Phys. Status Solidi C* **11**, 1296 (2014).